

Distribution-Guided and Constrained Quantum Machine Unlearning

Nausherwan Malik^a, Zubair Khalid^a, and Muhammad Faryad^{b,*}

^a*Department of Electrical Engineering, Lahore University of Management Sciences, Lahore 54792, Pakistan.*

^b*Department of Physics, Lahore University of Management Sciences, Lahore 54792, Pakistan.*

^{*}*muhammad.faryad@lums.edu.pk*

Abstract

Machine unlearning aims to remove the influence of specific training data from a learned model without full retraining. While recent work has begun to explore unlearning in quantum machine learning, existing approaches largely rely on fixed, uniform target distributions and do not explicitly control the trade-off between forgetting and retained model behaviour. In this work, we propose a distribution-guided framework for class-level quantum machine unlearning that treats unlearning as a constrained optimization problem. Our method introduces a tunable target distribution derived from model similarity statistics, decoupling the suppression of forgotten-class confidence from assumptions about redistribution among retained classes. We further incorporate an anchor-based preservation constraint that explicitly maintains predictive behaviour on selected retained data, yielding a controlled optimization trajectory that limits deviation from the original model. We evaluate the approach on variational quantum classifiers trained on the Iris and Covertype datasets. Results demonstrate sharp suppression of forgotten-class confidence, minimal degradation of retained-class performance, and closer alignment with the gold retrained model baselines compared to uniform-target unlearning. These findings highlight the importance of target design and constraint-based formulations for reliable and interpretable quantum machine unlearning.

1. Introduction

Machine Unlearning (MU), first introduced by [1] refers to removing the influence of specific data points from machine learning (ML) models without retraining the model from scratch. This is important for several reasons. Privacy regulations, such as the European Union’s (EU) General Data Protection Regulation (GDPR) require companies to delete user data on request from storage systems, as well as the influence of data points on model learning. Retraining models for each deletion is prohibitively expensive [2].

Unlearning also becomes necessary for security reasons. Contemporary adversarial attacks can introduce carefully crafted, misleading inputs that distort model behaviour, such as forcing the model to output incorrect health-care predictions. Additionally, where personalised systems adapt to user interests, an incorrect or accidental user action warrants immediate removal lest recommender systems continue to generate unwarranted suggestions [2]. ML models are also susceptible to training data bias, which enables them to discriminate against certain groups. [3] proposes the removal of certain attributes from the data

that are more prone to induce bias.

Quantum Machine Learning (QML) refers to algorithms designed to run on Quantum Computers [4]. With the increased traction of Quantum Machine Learning (QML) in recent years, data privacy, security, and protection remain a persistent issue. [5] design a Membership Inference Attack (MIA) tailored for QML models, demonstrating clear evidence of membership leakage from QML models. Their experiments validate Quantum Machine Unlearning (QMU) as a viable mechanism to resolve this issue. Considering the recent traction towards QML, there has been even less work in QMU.

Unlearning is generally achieved by either forgetting a certain class (Class Unlearning), forgetting specific data points (Instance Unlearning), or forgetting features of the data (Feature Unlearning). [6, 7, 8]

Very recently, [9] presented the first empirical study of MU in hybrid quantum-classical models, adapting a range of classical unlearning techniques to variational quantum circuits and proposing a complement-label strategy that enforces high-entropy predictions on forgotten samples. Their results demonstrate that quantum-enhanced mod-

els can support effective unlearning, with performance depending strongly on circuit depth and architectural choices.

In this work, we introduce a distribution-guided class unlearning framework for variational quantum classifiers that remove the predictive influence of a specified class without retraining from scratch. Our approach formulates unlearning as a constrained optimization problem that suppresses forgotten-class predictions while preserving the model’s behaviour on retained data through soft anchor constraints. Unlike existing unlearning methods that rely on uniform probability suppression or full data deletion, we construct a data-driven forget target distribution that redistributes probability mass according to the semantic similarity inferred from the original model’s outputs. The resulting objective admits a principled Lagrangian interpretation and is optimized directly at the level of quantum circuit parameters using parameter-shift gradients. We demonstrate that this approach achieves selective forgetting through localized parameter updates, maintains retained-class structure, and is effective across datasets of differing complexity, establishing a practical and theoretically grounded unlearning mechanism for near-term quantum machine learning models.

2. Theoretical Foundations

Machine unlearning refers to the removal of data and its corresponding influence from a trained machine learning model, without requiring full retraining from scratch. Let Z denote the space of all possible examples, and let Z^* denote the set of all finite datasets drawn from Z . Given a dataset $D \in Z^*$, a learning algorithm $A : Z^* \rightarrow H$ maps D to a hypothesis $A(D)$ in the hypothesis space H , which represents the set of admissible model parameters.

Given a trained model $A(D)$ and a subset of samples $D_f \subseteq D$ to be forgotten, an unlearning mechanism U takes as input $(D, D_f, A(D))$ and produces an updated model intended to approximate the counterfactual model obtained by training without D_f :

$$U(D_f, D, A(D)) \approx A(D \setminus D_f). \quad (1)$$

This formulation captures the central objective of MU: removing the functional influence of D_f while preserving the model’s performance on retained data.

[10] proposes two formal definitions of unlearning, which we summarise below.

2.1. Formal Definition 1

Given a learning algorithm $A(\cdot)$, a dataset D , and a forgotten subset $D_f \subseteq D$, an unlearning algorithm $U(\cdot)$ is said to perform *exact unlearning* if

$$\Pr(A(D \setminus D_f)) = \Pr(U(D, D_f, A(D))) = 1. \quad (2)$$

This definition emphasizes behavioural equivalence rather than procedural equivalence. The unlearning algorithm is not required to retrain the model from scratch, but rather to produce an outcome that is indistinguishable from retraining on $D \setminus D_f$. The probability measure captures stochasticity arising from initialization, data ordering, and optimization randomness.

2.2. Formal Definition 2

More generally, given a hypothesis space H , an unlearning algorithm U is said to perform exact unlearning if, for all measurable subsets $T \subseteq H$, datasets $D \in Z^*$, and forgotten subsets $D_f \subseteq D$,

$$\Pr(A(D \setminus D_f) \in T) = \Pr(U(D, D_f, A(D)) \in T). \quad (3)$$

Here, T represents a set of hypotheses satisfying certain structural or performance properties rather than a single parameter vector. Equality in distribution ensures that the unlearning procedure reproduces the same statistical behaviour as retraining, even if individual parameter realizations differ.

In practice, exact unlearning is often infeasible for modern models. Consequently, approximate unlearning techniques have been proposed, including variational Bayesian unlearning [11], which ensures that the posterior induced by unlearning remains close (in KL divergence) to the retrained posterior.

3. Quantum Machine Unlearning

QMU extends the classical unlearning paradigm to quantum and hybrid quantum-classical models. Unlike classical models parametrized in Euclidean space, quantum models are described by quantum states or density operators acting on Hilbert spaces. As a result, unlearning procedures must respect fundamental quantum constraints such as no-cloning and no-deletion.

[12] formalizes QMU as a contraction of distinguishability between the model state before unlearning and the counterfactual state obtained by excluding the forgotten

data. In this framework, an unlearning operation is modelled as a completely positive and trace-preserving (CPTP) map \mathcal{E} acting on the model state ρ . CPTP maps represent the most general physically realizable quantum transformations.

The contractivity of quantum channels implies that distinguishability between quantum states cannot increase under \mathcal{E} . This is formalized by the quantum data-processing inequality:

$$D(\rho\|\sigma) \geq D(\mathcal{E}(\rho)\|\mathcal{E}(\sigma)), \quad (4)$$

where $D(\cdot\|\cdot)$ denotes a suitable quantum divergence measure. In the context of unlearning, this inequality motivates viewing forgetting as a contractive reduction of data-dependent distinguishability, consistent with physically admissible quantum evolutions. Since quantum information cannot be deleted outright, QMU redistributes data-dependent information to the environment while preserving physical consistency. Accordingly, for variational quantum classifiers, contractivity is reflected in reduced distinguishability at the level of observable predictive distributions.

An effective QMU method should therefore satisfy three criteria: **efficiency**, requiring limited computational overhead; **completeness**, ensuring removal of the forgotten data's influence; and **verifiability**, providing measurable evidence of forgetting.

4. Methodology

We consider supervised three-class classification with four continuous input features and present a distribution-guided unlearning framework applicable to this setting. We instantiate the framework on two representative classification problems — one low-complexity (Iris) and one higher-complexity (Covertype) — to illustrate how the same unlearning objective behaves across regimes. For Covertype, classes 3, 5, and 7 are selected (remapped to 0,1,2), and the original 54-dimensional inputs are reduced to four dimensions via principal component analysis. Each input, in this case $x \in \mathbb{R}^4$, is min–max scaled to $[0, \pi]$ and embedded into a six-qubit variational quantum circuit. Features are encoded on qubits 0–3 using single-qubit rotations $R_y(x_i)$, with pairwise feature interactions introduced via entangling blocks of the form $\text{CX}(a, b) R_z(x_a x_b) \text{CX}(a, b)$ applied to qubit pairs (0, 1), (1, 2), and (2, 3). The feature map is reuploaded twice in

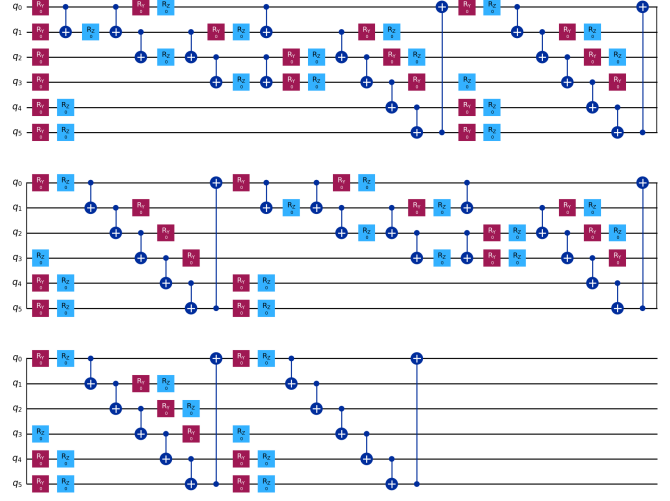


Figure 1: Variational quantum classifier architecture. A four-feature data-encoding map is reuploaded twice and interleaved with a hardware-efficient ansatz on six qubits. Features are embedded via single-qubit rotations and pairwise entangling blocks, followed by repeated layers of parametrized R_y – R_z rotations and ring CNOT entanglement. Pauli-Z expectation values on the readout qubits are used to produce class logits.

a layered feature map–ansatz–feature map–ansatz structure. The ansatz consists of ring entanglement with three repetitions. In each repetition, all six qubits undergo parametrised $R_y(\theta)$ and $R_z(\theta)$ rotations, followed by a ring of CNOT gates $\text{CX}(q, (q + 1) \bmod 6)$. This architecture results in 72 trainable parameters. Classification is performed by measuring Pauli-Z expectation values on qubits 3, 4, and 5, which are treated as logits and passed through a softmax to produce class probabilities. Model parameters are trained by minimizing the mini-batch cross-entropy loss using stochastic gradient-based optimization. Gradients with respect to each circuit parameter are estimated via the parameter-shift rule

$$\frac{\partial L(w)}{\partial w_i} = \frac{L(w + \frac{\pi}{2} e_i) - L(w - \frac{\pi}{2} e_i)}{2}, \quad (5)$$

where $L(w)$ denotes the mini-batch loss and e_i is the i -th standard basis vector. At each iteration, a mini-batch of 10 samples is drawn uniformly without replacement, and parameters are updated using Adam with a cosine learning-rate schedule over 300 iterations. Parameters are initialized with small Gaussian noise. The final model is selected by retaining the parameter configuration that achieves the lowest validation loss during training. Confusion matrices for Iris and Covertype classification after standard training are shown in Figures 2 and 3, respectively.

The formulation that follows depends only on the

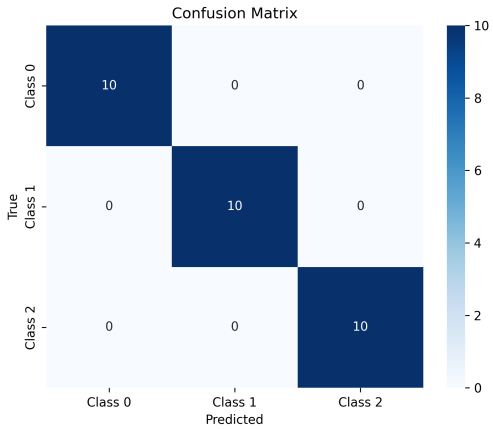


Figure 2: Confusion matrix for the Iris dataset after training the variational quantum classifier. Rows correspond to true class labels and columns to predicted labels. The model achieves near-perfect separation across all three classes.

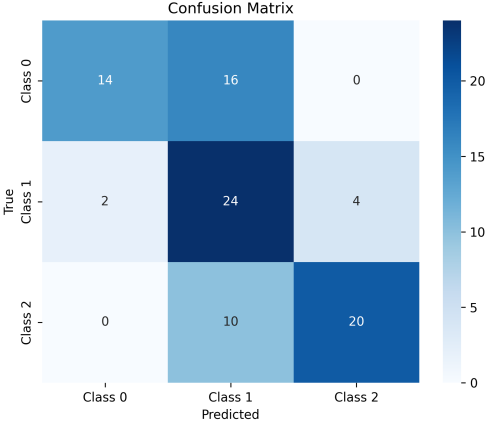


Figure 3: Confusion matrix for the Covertype dataset (classes 3, 5, and 7) after training. While correct predictions dominate the diagonal, residual confusion between classes reflects the increased complexity of the dataset compared to Iris.

model’s predictive distributions and parameter space, and does not rely on dataset-specific structure beyond a fixed classification setting. The proposed unlearning objective is defined at the level of output distributions and model parameters, and is independent of the particular dataset, feature embedding, or circuit architecture used to instantiate the classifier.

4.1. Distribution-Guided Class Unlearning

Let a trained classifier with parameters w_{orig} output a K -class predictive distribution $p_{w_{\text{orig}}}(y | x)$. Given a forgotten class f and a forget set F consisting of training samples with label f , our goal is to compute updated parameters w such that: (i) for inputs $x \in F$, the unlearned model assigns negligible probability to the forgotten class,

i.e., $p_w(f | x)$ is suppressed; and (ii) on the retained data, the model’s predictions remain close to the original model (and ideally close to a gold retrained model trained from scratch without F). In the following, we operationalize these objectives using a divergence-based forget loss on F and a constraint that preserves behaviour on a retained anchor set.

After standard training, we perform targeted class unlearning to remove predictive influence associated with a specified class f . To this end, the data are partitioned into a *forget set* F , containing samples associated with class f , and an *anchor set* A consisting of retained samples whose predictive behaviour should be preserved.

4.1.1. Distribution-Guided Forget Target

To guide the redistribution of probability mass during unlearning, we define a fixed target distribution $q \in \Delta^{K-1}$ satisfying $q_f = 0$. The remaining probability mass is distributed across non-forgotten classes according to the original model’s predictions on a calibration subset $S \subseteq F$ of the forget class. Specifically, we compute the mean softmax output of the original model on S and assign

$$q_k \propto (\mathbb{E}_{x \in S} [p_{w_{\text{orig}}}(k | x)])^\beta, \quad k \neq f, \quad (6)$$

followed by normalization. The exponent $\beta > 0$ controls the sharpness of the target distribution. This similarity-based construction redistributes probability mass according to the original model’s output distribution on the forget class, thereby favouring target classes that the model already considers similar. Consequently, probability mass is reassigned toward semantically proximate outputs rather than being uniformly distributed across all non-forgotten classes. Empirical evidence demonstrating the limitations of uniform redistribution, particularly in higher-complexity settings, is provided in [Appendix B](#). Because the target distribution in 6 is constructed solely from the model’s output probabilities on the forgotten class, the same procedure applies directly to any three-class classification task with continuous features, independent of the underlying dataset.

4.1.2. Anchor Reference Distributions

To preserve the model’s behaviour on retained data, we cache reference distributions $p_{w_{\text{orig}}}(\cdot | x)$ for all $x \in A$. Using soft reference distributions enables preservation of the relative class similarities and predictive calibration on anchor samples.

4.1.3. Unlearning Objective

Unlearning is performed by maximizing the following objective:

$$\begin{aligned} J(w) = & \mathbb{E}_{x \in F} \left[\sum_{k=1}^K q_k \log p_w(k \mid x) \right] \\ & + \alpha \mathbb{E}_{x \in A} \left[\sum_{k=1}^K p_{w_{\text{orig}}}(k \mid x) \log p_w(k \mid x) \right] \quad (7) \\ & - \lambda \|w - w_{\text{orig}}\|_2^2, \end{aligned}$$

where $\alpha \geq 0$ and $\lambda \geq 0$ are hyper-parameters. The first term encourages the model's predictions on the forget set to align with the similarity-guided target distribution q , which assigns zero probability to the forgotten class. The second term preserves the original model's predictive behaviour on anchor samples, while the final term penalizes large deviations from the original parameters.

4.1.4. Optimization and Interpretation

The objective in (7) is maximized via gradient ascent, using parameter-shift gradient estimates and optional mini-batching over the forget and anchor sets. A theoretical interpretation of this objective as a Lagrangian relaxation of a constrained unlearning problem is provided in Theorem 1, with proof deferred to [Appendix B](#).

Theorem 1 (Lagrangian formulation of distribution-guided unlearning). *Let $p_w(\cdot \mid x)$ denote the model softmax distribution induced by parameters w . Let F be a forget set and A be an anchor (retained) set. Let $p_{\text{ref}}(\cdot \mid x) := p_{w_{\text{orig}}}(\cdot \mid x)$ be the reference distribution produced by the original parameters w_{orig} on anchor samples. Let $q \in \Delta^{K-1}$ be a fixed target distribution satisfying $q_f = 0$ for the forgotten class f .*

Define

$$\begin{aligned} \mathcal{L}_F(w) &= \frac{1}{|F|} \sum_{x \in F} \sum_{k=1}^K q_k \log p_w(k \mid x), \\ \mathcal{L}_A(w) &= \frac{1}{|A|} \sum_{x \in A} \sum_{k=1}^K p_{\text{ref}}(k \mid x) \log p_w(k \mid x). \end{aligned}$$

Then, maximizing the objective

$$J(w) = \mathcal{L}_F(w) + \alpha \mathcal{L}_A(w) - \lambda \|w - w_{\text{orig}}\|_2^2, \quad \alpha, \lambda \geq 0, \quad (8)$$

is equivalent, up to additive constants independent of w , to maximizing the Lagrangian relaxation of the constrained

optimization problem

$$\begin{aligned} \max_w \quad & \mathcal{L}_F(w) \\ \text{such that} \quad & \frac{1}{|A|} \sum_{x \in A} \text{KL}(p_{\text{ref}}(\cdot \mid x) \parallel p_w(\cdot \mid x)) \leq \varepsilon, \quad (9) \\ & \|w - w_{\text{orig}}\|_2^2 \leq \rho, \end{aligned}$$

for some $\varepsilon, \rho \geq 0$.

4.2. Implementation Details

All experiments were implemented using Qiskit and executed on a noiseless statevector quantum simulator. Variational quantum classifiers were constructed using six qubits with data reuploading and a hardware-efficient ansatz composed of parametrised single-qubit rotations and nearest-neighbour entangling gates. Model outputs were obtained via exact expectation-value evaluation of Pauli-Z measurements on designated readout qubits, without shot noise or device-level errors. Gradients were computed using the parameter-shift rule, and optimization was performed using the Adam optimizer. No hardware noise models were assumed, as the focus of this work is on the algorithmic behaviour of quantum machine unlearning rather than device-specific performance.

4.3. Results

Unless stated otherwise, all unlearning experiments use $\alpha = 1.0$ and $\lambda = 0.01$ reflecting equal weighting of the forgetting and preservation terms, together with a mild quadratic anchoring to the original parameters. Targeted unlearning produces a sharp and selective degradation in performance for the forgotten class, while largely preserving retained-class behaviour, as shown in Figures 4 and 5. On Covertype, recall for the forgotten class decreases from 0.633 to 0.067, while recall for the two retained classes remains unchanged at 0.467 and 0.800, respectively. The mean predicted probability assigned to the forgotten class on its own data drops from 0.4055 to 0.2715, indicating a substantial reduction in residual confidence. For Iris, forgotten-class recall decreases from 1.000 to 0.000, while recall for class 0 remains at 1.000 and class 1 decreases modestly from 1.000 to 0.800. The corresponding forgotten-class mean probability decreases from 0.4155 to 0.2098. Across both datasets, post-unlearning confusion matrices show that errors introduced by unlearning primarily redistribute forgotten samples to a single retained class, consistent with similarity-guided probability reassignment rather than indiscriminate suppression.

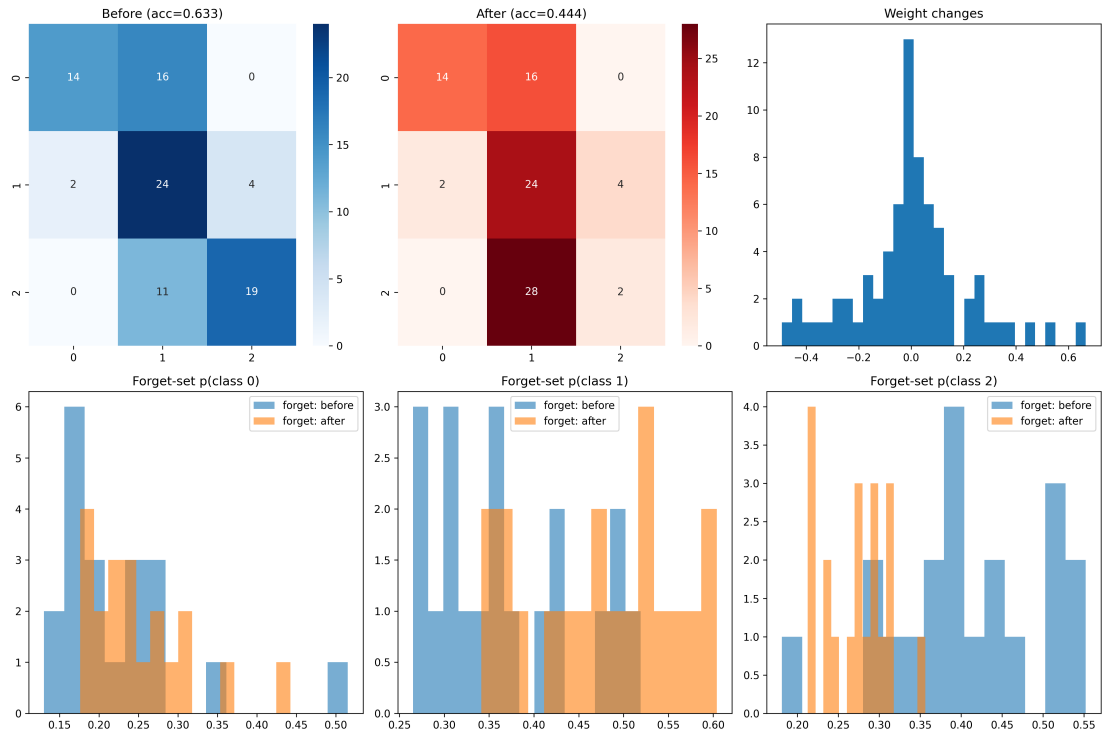


Figure 4: Confusion matrices before and after targeted unlearning on the Covertype dataset with class 2 forgotten. Predictions assigned to the forgotten class are strongly suppressed after unlearning, with errors primarily redistributing to a single retained class.

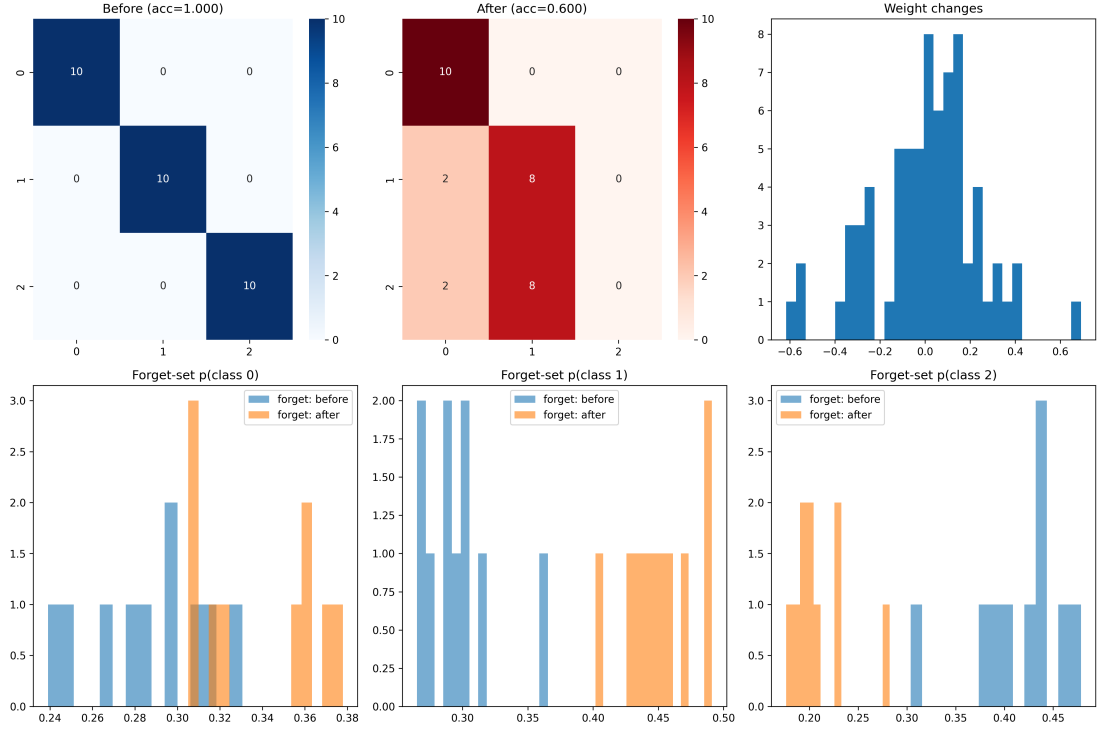


Figure 5: Confusion matrices before and after targeted unlearning on the Iris dataset with class 2 forgotten. Forgotten-class predictions are eliminated, while retained classes largely preserve pre-unlearning behaviour.

Table 1: Class-wise recall and forget-class confidence before and after unlearning. The forgotten class is class 2 in all experiments.

Dataset	Class	Recall (B)	Recall (A)	Δ Recall
Covertype	0	0.467	0.467	0.000
	1	0.800	0.800	0.000
	2 (F)	0.633	0.067	-0.566
Iris	0	1.000	1.000	0.000
	1	1.000	0.800	-0.200
	2 (F)	1.000	0.000	-1.000

Forget-class mean probability: Covertype 0.4055 → 0.2715, Iris 0.4155 → 0.2098.

Table 2: Divergence between gold retrained and unlearned models on retained test data. KL divergence computed after renormalizing over retained labels only. Lower values indicate closer agreement.

Dataset	Ret. Labels	Mean KL	Med. KL	Max KL
Covertype	{0,1}	0.0468	0.0342	0.1625

Mean prob. on forgotten class (retained samples): Gold 0.195, Unlearned 0.295.

Beyond accuracy-based metrics, we evaluate how closely the unlearned model approximates true retraining by comparing its predictive distributions to those of a gold retrained model trained on retained data only. We compute the Kullback–Leibler (KL) divergence between the gold retrained and unlearned predictive distributions on retained-class test samples. Probabilities are renormalized over retained labels to exclude trivial effects from probability mass assigned to the forgotten class. This ensures that divergence reflects agreement on retained-class behaviour rather than the degree of forgetting itself. This comparison serves as an empirical proxy for distributional equivalence in Definition 2, assessing whether unlearning reproduces the statistical behaviour of retraining on retained data.

On the Covertype dataset, the unlearned model achieves a mean KL divergence of 0.047 ± 0.047 relative to the gold retrained model, with a median of 0.034. This low divergence indicates that, despite aggressive suppression of the forgotten class, the unlearned model closely matches the behaviour of a model trained from scratch on retained data. At the same time, the unlearned model assigns a larger fraction of probability mass to the forgotten class than the gold-retrained model on retained samples (0.295 vs. 0.195), reflecting a mild under-learning that does not substantially affect retained-class predictions. While our experiments focus on class unlearning, extending similarity-guided and constraint-based formulations to instance-level unlearning remains an important direction for future work.

5. Conclusions

We introduced a generalised four-feature three-class distribution-guided and constrained framework for quantum machine unlearning that selectively suppresses forgotten-class influence while preserving retained behaviour. Experiments on variational quantum classifiers demonstrate sharp forgetting, minimal degradation on retained classes, and close alignment with gold retraining baselines. From a quantum information perspective, our framework is motivated by physical admissibility constraints on unlearning operations. In practice, we realize these principles through constrained variational optimization, with unlearning quality evaluated empirically via alignment to gold retraining.

Data Availability

All data generated or analysed during this study are included in this published article and the accompanying figures. The code supporting the findings of this study will be made publicly available at github.com/nausherwan-malik/Distribution-Guided-Constrained-Quantum-Machine-Unlearning.

Author Contributions

NM designed and implemented the proposed methodology; conducted all experiments and data analysis; and wrote the draft of the manuscript. MF proposed the research idea, supervised the project and data analysis, and guided the writing of the manuscript. ZK supervised the research and provided oversight and feedback on the study. All authors reviewed and approved the final version of the manuscript.

References

- [1] Y. Cao, J. Yang, Towards making systems forget with machine unlearning, in: 2015 IEEE Symposium on Security and Privacy, IEEE, 2015.
- [2] T. T. Nguyen, T. T. Huynh, Z. Ren, P. L. Nguyen, A. W.-C. Liew, H. Yin, Q. V. H. Nguyen, [A survey of machine unlearning](#), arXiv preprint (2024). [arXiv:2209.02299](https://arxiv.org/abs/2209.02299).
URL <https://arxiv.org/abs/2209.02299>

[3] W. Wang, Z. Tian, C. Zhang, S. Yu, [Machine unlearning: A comprehensive survey](#), arXiv preprint (2024). [arXiv:2405.07406](#).
URL <https://arxiv.org/abs/2405.07406>

[4] G. Sergioli, [Quantum and quantum-like machine learning: a note on differences and similarities](#), Soft Computing 24 (2020) 10247–10255. [doi:10.1007/s00500-019-04429-x](#).
URL <https://doi.org/10.1007/s00500-019-04429-x>

[5] J. Su, R. He, G. Li, S. Qin, Z. He, H. Situ, F. Gao, [From membership-privacy leakage to quantum machine unlearning](#), arXiv preprint arXiv:2509.06086State Key Laboratory of Networking and Switching Technology, Beijing University of Posts and Telecommunications, Beijing, China (2025).
URL <https://arxiv.org/abs/2509.06086>

[6] L. Bourtoule, V. Chandrasekaran, C. A. Choquette-Choo, H. Jia, A. Travers, B. Zhang, D. Lie, N. Paepernot, Machine unlearning, in: 2021 IEEE Symposium on Security and Privacy (SP), 2021, pp. 141–159. [doi:10.1109/SP40001.2021.00019](#).

[7] D. Zagardo, [A more practical approach to machine unlearning](#) (2024). [arXiv:2406.09391](#).
URL <https://arxiv.org/abs/2406.09391>

[8] D. Trippa, C. Campagnano, M. S. Bucarelli, G. Tolomei, F. Silvestri, [\$\nabla\tau\$: Gradient-based and task-agnostic machine unlearning](#) (2024). [arXiv:2403.14339](#).
URL <https://arxiv.org/abs/2403.14339>

[9] C. Crivoi, R. T. Ionescu, [Machine unlearning in the era of quantum machine learning: An empirical study](#) (2025). [arXiv:2512.19253](#).
URL <https://arxiv.org/abs/2512.19253>

[10] C. Li, H. Jiang, J. Chen, Y. Zhao, S. Fu, F. Jing, Y. Guo, An overview of machine unlearning, High-Confidence Computing 5 (2025) 100254.

[11] Q. P. Nguyen, B. K. H. Low, P. Jaillet, [Variational bayesian unlearning](#) (2020). [arXiv:2010.12883](#).
URL <https://arxiv.org/abs/2010.12883>

Appendix A. Limitations of uniform forget-target assignment

Figure A.6 illustrates the effect of assigning a uniform target distribution over non-forgotten classes during unlearning on the Covertype dataset. While uniform redistribution reduces the model’s confidence in the forgotten class, the suppression is substantially weaker than under similarity-guided targets, with the mean forgotten-class probability decreasing only from 0.405 to 0.373. Class-wise confusion matrices show that a large fraction of forgotten samples continue to be predicted as the forgotten class after unlearning, and the overall accuracy remains relatively high at 0.578, indicating incomplete forgetting. Moreover, probability mass is redistributed diffusely across retained classes rather than concentrating on a semantically proximate class, leading to less structured confusion patterns. These results highlight that uniform target assignment fails to sufficiently remove class-specific predictive influence in more complex datasets, motivating the use of similarity-informed targets.

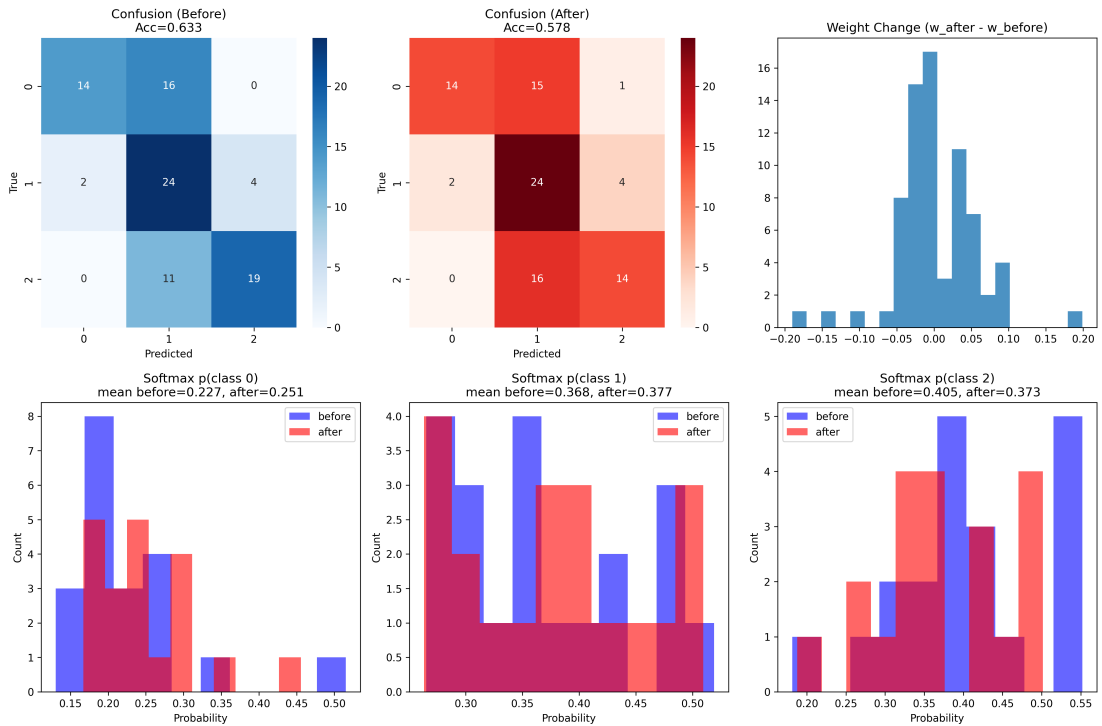


Figure A.6: Effect of uniform forget-target assignment on the Covertype dataset. The confusion matrices show model predictions before (left) and after (center) unlearning using a uniform target distribution over non-forgotten classes, while the right panel reports the distribution of parameter changes. Uniform redistribution reduces, but does not eliminate, predictions assigned to the forgotten class, with the mean forgotten-class probability decreasing from 0.405 to 0.373. Probability mass is dispersed across retained classes rather than concentrated on a semantically similar class, resulting in less structured post-unlearning confusion patterns compared to similarity-guided unlearning.

Appendix B. Proof of Theorem 1

For any anchor sample $x \in A$,

$$\sum_k p_{\text{ref}}(k \mid x) \log p_w(k \mid x) = -\text{KL}(p_{\text{ref}}(\cdot \mid x) \parallel p_w(\cdot \mid x)) + \sum_k p_{\text{ref}}(k \mid x) \log p_{\text{ref}}(k \mid x),$$

where the second term does not depend on w . Averaging over $x \in A$ yields

$$\mathcal{L}_A(w) = -\frac{1}{|A|} \sum_{x \in A} \text{KL}(p_{\text{ref}}(\cdot \mid x) \parallel p_w(\cdot \mid x)) + C,$$

for a constant C independent of w . Substituting this expression into (8) and discarding constants independent of w gives

$$J(w) \equiv \mathcal{L}_F(w) - \alpha \frac{1}{|A|} \sum_{x \in A} \text{KL}(p_{\text{ref}}(\cdot | x) \| p_w(\cdot | x)) - \lambda \|w - w_{\text{orig}}\|_2^2.$$

This expression is precisely the Lagrangian associated with the constrained optimization problem in (9), with Lagrange multipliers α and λ , completing the proof.

Appendix C. Ablation Studies

This appendix investigates the sensitivity of the proposed distribution-guided quantum machine unlearning framework to its principal design choices and hyperparameters. Given that the Iris dataset is a simple, low-complexity classification task, all ablations are conducted on the Covertype dataset using the variational quantum classifier described in Section 4.1, unless stated otherwise. Unless varied explicitly, the default unlearning parameters are $\alpha = 1.0$, $\lambda = 0.01$, and $\beta = 1.0$. To avoid repeating the class unlearning discussed in the previous discussions, we exclude unlearning in class 2 in these experiments.

Throughout this appendix, forgetting effectiveness is quantified by the mean predicted probability assigned to the forgotten class on its own samples, while retained utility is measured by test accuracy on all classes.

Appendix C.1. Class-wise forgetting robustness

We first evaluate whether the proposed method depends on the specific choice of forgotten class. Using the default unlearning configuration, we apply class-level unlearning to each non-trivial class in turn and report the resulting forgetting strength and retained accuracy.

Table C.3: Class-wise unlearning performance on Covertype. Results are reported for non-trivial forgotten classes. Lower forgotten-class probability indicates stronger forgetting.

Forgotten Class	Test Acc. (Before)	Test Acc. (After)	p_f (After)
0	0.633	0.411	0.260
1	0.633	0.411	0.261

Across forgotten classes, the method consistently suppresses confidence assigned to the forgotten class while maintaining comparable retained accuracy. This indicates that the unlearning behaviour is not specific to a single class choice and is robust across non-trivial forgetting scenarios.

Appendix C.2. Sensitivity to similarity sharpness β

The distribution-guided target distribution in Eq. (6) depends on the sharpness parameter β , which controls how strongly the probability mass is concentrated on the most semantically similar retained class. We sweep $\beta \in \{0.25, 0.5, 0.75, 1.0\}$ while keeping all other parameters fixed.

Table C.4: Effect of varying the similarity sharpness parameter β on forgetting and retention.

β	Test Acc. (After)	p_f (After)
0.25	0.400	0.269
0.50	0.411	0.267
0.75	0.422	0.264
1.00	0.411	0.261

Performance varies smoothly with β , with no sharp degradation in either forgetting or retaining accuracy. This indicates that the similarity-guided target construction is robust to moderate changes in sharpness, and does not require precise tuning.

Appendix C.3. Anchor set size sensitivity

We next examine how the size of the retained anchor set affects unlearning performance. The anchor set is subsampled in a stratified manner to preserve class balance, using fractions $\{10\%, 25\%, 50\%, 100\%\}$ of the original anchor data.

Table C.5: Effect of anchor set size on unlearning performance.

Anchor Fraction	Test Acc. (After)	p_f (After)
0.10	0.356	0.250
0.25	0.411	0.260
0.50	0.422	0.260
1.00	0.411	0.261

Retention performance improves rapidly as the anchor fraction increases from 10% to 25% and stabilizes thereafter, while forgetting effectiveness remains largely unchanged. This suggests that only a modest retained anchor subset is sufficient to preserve model behaviour, highlighting the practical efficiency of the proposed constraint.

Appendix C.4. Effect of anchor-preservation weight α

The coefficient α in Eq. (7) controls the strength of the anchor-preservation term. To assess its role, we vary $\alpha \in \{0, 1, 2\}$ while keeping all other parameters fixed.

Table C.6: Effect of varying α on forgetting and retention.

α	Test Acc. (After)	p_f (After)
0	0.300	0.214
1	0.411	0.261
2	0.400	0.270

Removing the anchor constraint ($\alpha = 0$) leads to aggressive forgetting but substantial degradation of retained accuracy. Increasing α moderates forgetting while improving retention, consistent with the Lagrangian interpretation of Theorem 1.

Appendix C.5. Effect of parameter anchoring λ

Finally, we study the effect of the quadratic parameter anchoring term in Eq. (7) by varying $\lambda \in \{0, 0.01, 0.1\}$.

Table C.7: Effect of varying the parameter anchoring coefficient λ .

λ	Test Acc. (After)	p_f (After)
0	0.411	0.251
0.01	0.411	0.261
0.10	0.433	0.334

Larger values of λ improve retention at the cost of weaker forgetting, while $\lambda = 0$ retains effective forgetting but provides less stability. This confirms that parameter anchoring acts as a secondary stabilization mechanism, complementing the anchor distribution constraint rather than replacing it.

Summary. Across all ablations, the proposed distribution-guided and constrained unlearning framework exhibits stable and interpretable behaviour. The method is robust to the choice of forgotten class, insensitive to moderate changes in the similarity sharpness parameter, and requires only a modest anchor subset to preserve retained behaviour. The effects of α and λ align closely with the Lagrangian interpretation of the objective, providing empirical validation of the theoretical formulation in Section 4.1.